Mechanical disruption of E-cadherin complexes with epidermal growth factor receptor actuates growth factor–dependent signaling

Brendan Sullivan[a], Taylor Light[b], Vinh Vu[a], Adrian Kapustka[a], Kalina Hristova[b,1], and Deborah Leckband[a,c,d,e,1]

[a]Department of Biochemistry, University of Illinois at Urbana–Champaign, Urbana, IL 61801; [b]Department of Materials Science and Engineering, Institute for NanoBioTechnology, Johns Hopkins University, Baltimore, MD 21218; [c]Department of Chemistry, University of Illinois at Urbana–Champaign, Urbana, IL 61801; [d]Department of Chemical and Biomolecular Engineering, University of Illinois at Urbana–Champaign, Urbana, IL 61801; and [e]Center for Quantitative Biology and Biophysics, University of Illinois at Urbana–Champaign, Urbana, IL 61801

Edited by Joan Brugge, Department of Cell Biology, Harvard Medical School, Boston, MA; received January 12, 2021; accepted December 10, 2021

Increased intercellular tension is associated with enhanced cell proliferation and tissue growth. Here, we present evidence for a force-transduction mechanism that links mechanical perturbations of epithelial (E)-cadherin (CDH1) receptors to the force-dependent activation of epidermal growth factor receptor (EGFR, ERBB1)—a key regulator of cell proliferation. Here, coimmunoprecipitation studies first show that E-cadherin and EGFR form complexes at the plasma membrane that are disrupted by either epidermal growth factor (EGF) or increased tension on homophilic E-cadherin bonds. Although force on E-cadherin bonds disrupts the complex in the absence of EGF, soluble EGF is required to mechanically activate EGFR at cadherin adhesions. Fully quantified spectral imaging fluorescence resonance energy transfer further revealed that E-cadherin and EGFR directly associate to form a heterotrimeric complex of two cadherins and one EGFR protein. Together, these results support a model in which the tugging forces on homophilic E-cadherin bonds trigger force-activated signaling by releasing EGFR monomers to dimerize, bind EGF ligand, and signal. These findings reveal the initial steps in E-cadherin–mediated force transduction that directly link intercellular force fluctuations to the activation of growth regulatory signaling cascades.

cadherin | epidermal growth factor receptor | mechanotransduction | FRET | MAPK

Identifying force-transduction mechanisms is key to understanding the impact of mechanical cues on physiology. Force fluctuations influence diverse biological processes that include convergence extension movements (1), cell shape control (2), and the regulation of vascular permeability and inflammation (3–5). It is also well established that altered mechanical inputs affect growth-regulatory signaling. In epithelia, changes in cytoskeletal mechanics affect cell proliferation and tissue growth through the tension-dependent regulation of the Hippo pathway (6, 7). Increased intercellular tension in epithelia sensitizes cells to lower epidermal growth factor (EGF) concentrations (8), and mechanically stretching kidney epithelial monolayers triggered cell cycle entry (9). In three-dimensional (3D) cultures, higher luminal pressure in epithelial acini drives morphogenesis and increases proliferation (10, 11). In vivo, changes in tension in the imaginal disk affect *Drosophila* wing disk size (12, 13). Although integrin force sensing may contribute to these processes (14, 15), intercellular adhesion proteins are also important force transduction hubs (5, 16, 17).

Classical cadherins are major adhesion and mechanotransduction loci at intercellular junctions (18–21). The extracellular domains mediate intercellular adhesion, and the intracellular domain is mechanically coupled to the actin cytoskeleton through the cytosolic adaptor proteins α− and β−catenin (22). One established, cadherin-mediated force transduction mechanism involves α−catenin, which links cadherin complexes to actin filaments (16). Under tension, α−catenin undergoes a conformation change, which exposes a cryptic vinculin binding site that scaffolds local cytoskeletal remodeling (16, 23). Activated α−catenin also appears to recruit Ajuba family proteins, which suppress Hippo signaling and promote proliferation (6, 7, 13).

An additional force transduction mechanism identified at interepithelial junctions involves the epidermal growth factor receptor (EGFR). Mechanically perturbed E-cadherin complexes activate EGFR signaling through an EGF-dependent mechanism (24, 25). The resulting kinase cascade in turn activates integrins, increases cell contractility and cell stiffness, and regulates the recruitment of vinculin and actin to perturbed cadherin adhesions (25). This pathway connects E-cadherin tugging forces to EGFR activation, but how?

There is evidence that E-cadherin directly associates with and alters EGFR signaling. Crosstalk between E-cadherin and EGFR regulates density-dependent growth, in "contact-inhibited proliferation" (26–29). Intercellular adhesion down-regulates growth-regulatory signals through cross talk with EGFR and colocalization at the basolateral plane (6, 26, 30, 31).

Significance

Force transduction at interepithelial junctions involves E-cadherin–mediated activation of epidermal growth factor receptor (EGFR) signaling, which modulates local cytoskeletal remodeling and cell proliferation. Findings show that E-cadherin and EGFR form a heteroreceptor complex at the membrane. Increased tension on E-cadherin bonds disrupts the complex in the absence of epidermal growth factor (EGF), but the mechanical activation of EGFR signaling requires soluble EGF. Fully quantified spectral imaging fluorescence resonance energy transfer measurements further revealed that E-cadherin and EGFR form a heterotrimeric complex at the plasma membrane, comprising two E-cadherins bound to an EGFR monomer. These results suggest that tugging forces on E-cadherin adhesions activate force transduction cascades, by releasing EGFR monomers from the complex, to enable EGFR to homodimerize, bind EGF, and signal.

Author contributions: B.S., T.L., V.V., K.H., and D.L. designed research; B.S., T.L., V.V., A.K., K.H., and D.L. performed research; T.L., K.H., and D.L. contributed new reagents/analytic tools; B.S., T.L., A.K., K.H., and D.L. analyzed data; and B.S., T.L., K.H., and D.L. wrote the paper.

The authors declare no competing interest.

This article is a PNAS Direct Submission.

[1]To whom correspondence may be addressed. Email: kalina.hristova@jhu.edu or leckband@illinois.edu.

This article contains supporting information online at http://www.pnas.org/lookup/suppl/doi:10.1073/pnas.2100679119/-/DCSupplemental.

Published January 24, 2022.

BIOPHYSICS AND COMPUTATIONAL BIOLOGY

Prior coimmunoprecipitation (Co-IP) results suggested that E-cadherin and EGFR associate via their extracellular domains (29, 32). Point mutations in the E-cadherin ectodomain are linked to hereditary diffuse gastric cancer and increase EGFR phosphorylation at intercellular adhesions (33). Although some findings suggest direct receptor interactions, others suggest indirect protein coupling; the tumor suppressor Merlin regulates contact-dependent proliferation and couples EGFR to α−catenin (34). Determining how force and EGF alter the complexes, whether E-cadherin and EGFR directly associate, and the complex stoichiometry is central to identifying the early initial steps in E-cadherin force transduction signaling.

Results from this study provide molecular details of the complex between E-cadherin and EGFR and its regulation by EGF and force. Co-IP and use of mechanical perturbations revealed that E-cadherin and EGFR form a heteroreceptor complex that is disrupted by tension on homophilic E-cadherin bonds, in the presence and absence of soluble EGF. However, force-activated EGFR signaling requires EGF (24, 25). Results also expose the distinct contributions of integrins and E-cadherin to the mechanical activation of growth factor receptor signaling and downstream Erk1/2 activation. To further investigate details of the receptor interactions, we used fully quantified spectral imaging fluorescence resonance energy transfer (FSI-FRET) measurements (35). Results show that E-cadherin and EGFR form a heterotrimeric complex at the plasma membranes of live cells. This complex stoichiometry provides insight into how E-cadherin can mechanically regulate EGFR signaling. Together, findings reveal initial molecular events in E-cadherin–mediated force-transduction signaling.

Results

EGF Treatment Reduces E-Cadherin/EGFR Complex Levels. Co-IP measurements confirmed E-cadherin/EGFR heterocomplex formation. Studies used A-431D epithelial cells that were engineered to stably express human E-cadherin (A-431D$^{E\text{-}cad}$). The parental A-431D line does not express E-cadherin, but it overexpresses EGFR (36). We also used MCF-10A cells—an extensively used human breast epithelial line that expresses normal levels of EGFR and E-cadherin. Fig. 1 shows E-cadherin/EGFR complex levels in the absence and presence of EGF. In A-431D$^{E\text{-}cad}$ cells, the proteins coimmunoprecipitate in the absence of EGF (Fig. 1 *A* and *B*), but treatment with 20 nM EGF (>K_d ~2 nM) for 15 min decreased complex levels significantly (Fig. 1 *A* and *B*). These results were the same, whether determined by EGFR (Fig. 1*A*) or by E-cadherin (Fig. 1*B*) pulldown. Fig. 1*C* shows the quantified changes, normalized by the intensities for untreated cells. Results obtained with MCF-10A cells were similar. The receptors coimmunoprecipitate (Fig. 1 *D* and *E*), and 20 nM EGF reduces the complex levels when assessed by EGFR (Fig. 1 *D* and *F*) or by E-cadherin pull down (Fig. 1 *E* and *F*).

We further tested how EGF at concentrations near the K_d (~2 nM) affects complex disruption. Co-IP levels assessed at 5 and 15 min after treatment with 3 nM EGF (*SI Appendix*, Fig. S1*A*) showed little disruption at 5 min but significant reduction after 15 min (*SI Appendix*, Fig. S1*B*). The kinetics are slower than in some reports, where much higher EGF concentrations (15 to 280 nM) caused significant EGFR internalization and signaling within ~5 min (33, 34, 37, 38). However, consistent with our observations, changes in phosphorylated YAP or Erk were observed ~30 min after treatment with 1 to 2 nM EGF (28, 39). Based on kinetic arguments, rates of internalization and signaling might be expected to decrease with ligand (EGF) concentration. One reason for using low EGF concentrations was to slow the rate of complex disruption to enable studies of combined effects of stretch and EGF that require longer measurement times.

Increased Junction Tension Disrupts E-Cadherin/EGFR Complexes, Independent of EGF. Prior reports showed that tugging on E-cadherin receptors triggers EGFR-dependent signaling and adaptive cell stiffening in an EGF-dependent manner (24, 25). Here, studies first tested how E-cadherin tension affects the heteroreceptor complex, by quantifying the effect of 10% substrate

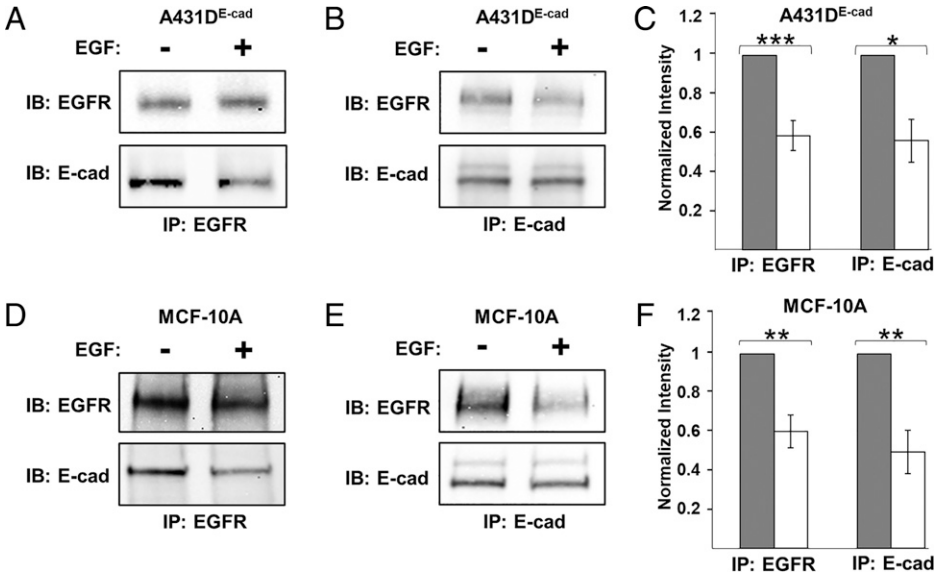

Fig. 1. Soluble EGF disrupts E-cadherin/EGFR complexes. (*A* and *B*) Co-IP results of EGFR and E-cadherin obtained with A-431D$^{E\text{-}cad}$ monolayers. Cells were seeded on PDMS membranes coated with fibronectin and cultured in reduced serum (0.5 vol%) for 24 h prior to treatment with 20 nM EGF for 15 min. Controls were not treated with EGF. Lysates were pulled down with (*A*) anti-EGFR antibody or (*B*) anti–E-cadherin and probed for respectively, E-cadherin or EGFR. (*C*) Quantified, normalized band intensities obtained under conditions in panel *A* ($n = 4$) and panel *B* ($n = 3$). Results were normalized by the band intensities in untreated samples. (*D* and *E*) Co-IP measurements of MCF-10A monolayers. Immunoprecipitation was done with either (*D*) anti-EGFR or (*E*) anti–E-cadherin antibody. (*F*) Band intensities, normalized as in panel *C*, were determined for anti-EGFR ($n = 3$) and anti-E-cadherin ($n = 4$) pulldowns. Error bars are SEM. *$P < 0.05$, **$P < 0.005$, ***$P < 0.0005$.

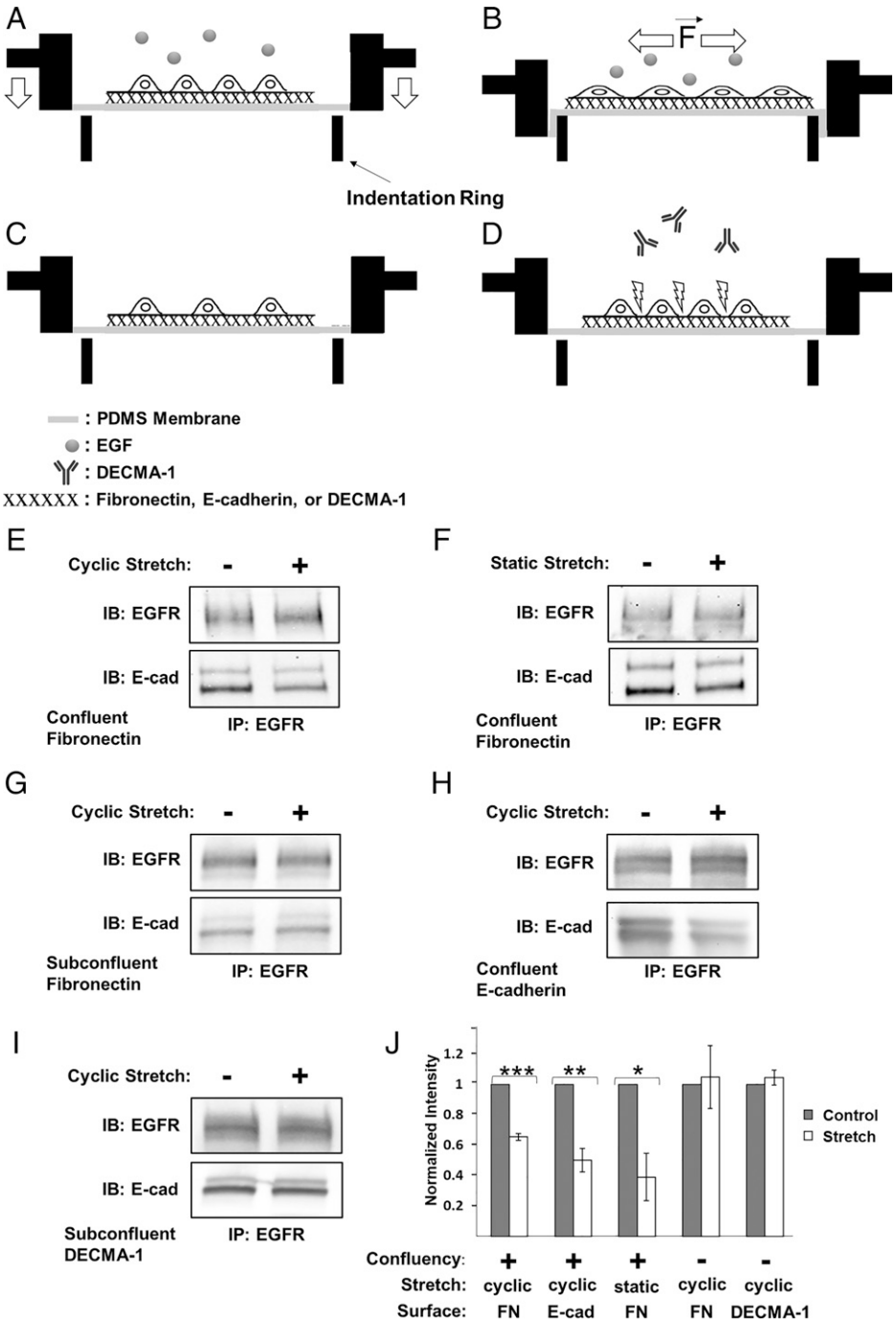

Fig. 2. Mechanically perturbing E-cadherin receptors disrupts E-cadherin/EGFR complexes, independent of EGF. (*A–D*) Experimental stretcher design and configurations used to apply equibiaxial strain to cells. (*A* and *B*) Confluent monolayers are cultured on PDMS membranes coated with either fibronectin, E-cad-Fc, or DECMA-1. Studies are done in the absence or presence of soluble EGF. (*B*) Membranes and overlying cell layers are stretched by pulling the membrane over an indenter ring (74). Other configurations used include (*C*) subconfluent cells on protein-coated membranes or (*D*) confluent monolayers on fibronectin, treated with E-cadherin blocking antibody, DECMA-1. Panels *E–I*, were obtained with serum-starved A-431D$^{E\text{-}cad}$ cells treated with neutralizing anti-EGF antibody prior to applying 10% strain for 30 min. 16G3 antibody was added to all samples not seeded on fibronectin. Co-IP results obtained with (*E*) cyclically or (*F*) statically stretched confluent cell monolayers on fibronectin. (*G*) Co-IP results for cyclically stretched subconfluent culture on fibronectin. (*H*) Co-IP results of cyclically stretched confluent cells on E-cad-Fc–coated PDMS membranes. (*I*) Co-IP measurements done with subconfluent cells on DECMA-1–coated membranes (*J*) Normalized E-cadherin band intensities measured following cyclic ($n = 4$) or static ($n = 3$) monolayer stretching on fibronectin or E-cad-Fc ($n = 3$)–coated membranes. Cyclically stretched subconfluent A-431D$^{E\text{-}cad}$ cells seeded on fibronectin ($n = 3$) or DECMA-1 ($n = 4$) are also included. The band intensities are normalized by the EGFR band intensities of untreated cells (gray bars). The white bars indicate the normalized Co-IP data from stretched cells. Error bars are SEM. *$P = 0.05$, **$P = 0.005$, ***$P = 0.0005$.

strain on E-cadherin/EGFR Co-IP levels, in the absence of EGF. Confluent A-431D$^{E\text{-}cad}$ monolayers (Fig. 2*A*) were serum starved and treated with EGF-neutralizing antibody. After 30 min of 10% cyclic stretch on fibronectin, the complex levels decreased significantly (Fig. 2 *E* and *J*). We also determined E-cadherin/EGFR complex levels following 30 min of 10% static strain.

BIOPHYSICS AND COMPUTATIONAL BIOLOGY

When confluent A-431D$^{E\text{-}cad}$ monolayers were stretched and held, complex levels also decreased significantly relative to unperturbed cells (Fig. 2 *F* and *J*). Results obtained with MCF-10A monolayers subject to 10% cyclic strain were similar (*SI Appendix*, Fig. S1 *C* and *D*).

To confirm that complex disruption was caused by increased tension on cadherin adhesions and not by other stretch-related signaling, subconfluent A-431D$^{E\text{-}cad}$ cells on fibronectin-coated poly(dimethylsiloxane) (PDMS) (Fig. 2*C*) were also subjected to 10% cyclic stretch for 30 min. Stretching subconfluent monolayers had no significant effect on E-cadherin/EGFR complex levels (Fig. 2 *G* and *J*). To further test whether tension on cadherin adhesions disrupts the heterocomplex, we stretched confluent A-431D$^{E\text{-}cad}$ cells on Fc-tagged E-cadherin extracellular domains (E-cad-Fc) (Fig. 2 *A* and *H*). This also reduced complex levels (Fig. 2 *H* and *J*), as did perturbing subconfluent cells on E-Cad-Fc (*SI Appendix*, Fig. S1 *E* and *F*). Thus, increased tension on homophilic cadherin bonds is sufficient to disrupt the E-cadherin/EGFR complex, in the absence of EGF.

Results suggest that E-cadherin–based mechanotransduction requires homophilic ligation (40, 41). To determine whether simply tugging on E-cadherin receptors is sufficient to dissociate the heterocomplex, A-431D$^{E\text{-}cad}$ cells were seeded at subconfluent density (Fig. 2*C*) on membranes coated with the anti–E-cadherin antibody, DECMA-1. Cells were allowed to attach for 5 h in the presence of anti-fibronectin 16G3 and EGF-neutralizing antibodies. During stretch, cells remained attached to the substrates (*SI Appendix*, Fig. S2), and stretch had no significant effect on complex levels (Fig. 2 *I* and *J*). Thus, merely tugging on E-cadherin is not sufficient to mechanically disrupt E-cadherin/EGFR complexes. Complex disruption requires homophilic cadherin ligation.

EGF and Junctional Tension Cooperate to Disrupt E-Cadherin/EGFR Complexes. Studies tested whether EGF and stretch cooperate to disrupt cadherin/EGFR complexes, by stretching confluent monolayers in the presence or absence of EGF. Studies used 3 nM EGF to prevent complete complex disruption by EGF alone (*SI Appendix*, Fig. S1 *A* and *B*). Treatment with 3 nM EGF reduced E-cadherin/EGFR complex levels, relative to untreated confluent monolayers on either E-cad-Fc (Fig. 3 *A* and *B*) or fibronectin (Fig. 3 *C* and *D*)-coated substrates. This agreed with prior reports (42). In the presence of 3 nM EGF, stretching confluent A-431D$^{E\text{-}cad}$ monolayers for 30 min further decreased heterocomplex levels, relative to EGF treatment alone (Fig. 3 *B* and *D*). These findings indicate that junctional tension and soluble EGF additively disrupt E-cadherin/EGFR complexes.

Mechanically Perturbed E-Cadherin Potentiates EGF-Dependent EGFR Activation. Studies next tested the impact of increased E-cadherin tension on EGFR phosphorylation. However, integrins also activate EGFR through an EGF-independent mechanism involving Src kinase (43). Conversely, E-cadherin–mediated force transduction requires EGF (Fig. 3) (25). These differences enabled us to distinguish between integrin and cadherin contributions in stretched, confluent monolayers.

To eliminate integrin interference and isolate the E-cadherin contribution, cells were seeded on membranes coated with E-cad-Fc. Fibronectin blocking antibody 16G3 was included to block integrin adhesion to secreted fibronectin. Controls used the nonbinding isotype 13G12. Confluent epithelial monolayers adhered to the E-cad-Fc–coated membranes and remained intact during cyclic stretching (*SI Appendix*, Fig. S2). Cells were subjected to four conditions: ±30 min of 10% stretch, ± 3 nM EGF

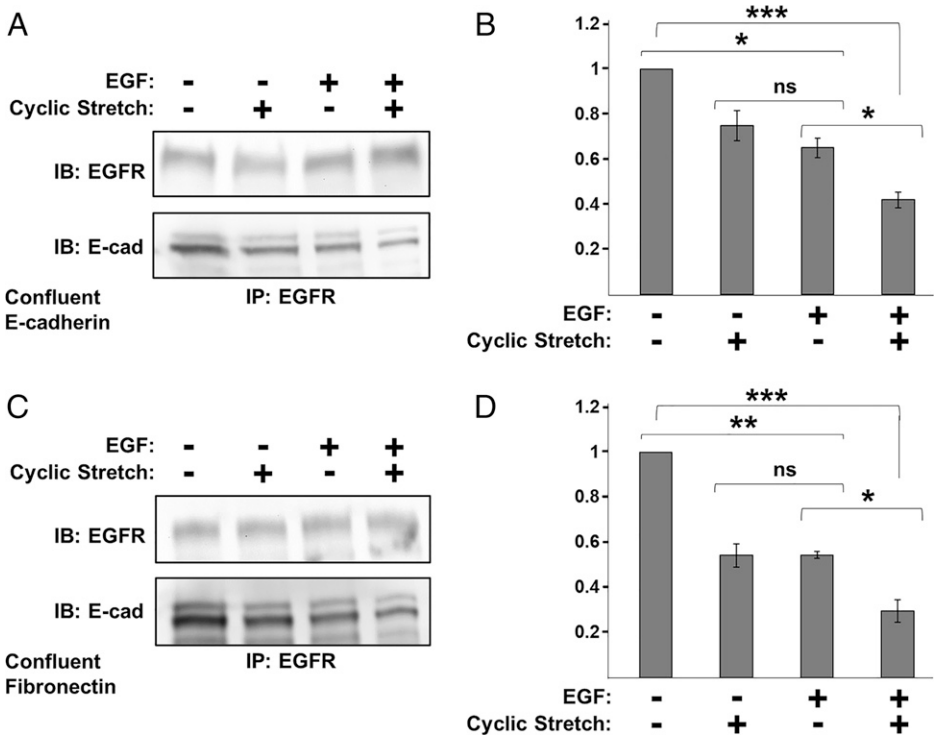

Fig. 3. EGF and cyclic stretch cooperate to disrupt E-cadherin/EGFR complexes. Co-IP results obtained with 24 h serum-starved confluent A-431D$^{E\text{-}cad}$ monolayers subjected to four conditions: ±3 nM EGF and ±10% cyclic stretch for 30 min. EGF-neutralizing antibody was added to all samples not treated with EGF. (*A*) Co-IP results for monolayers seeded on E-cad-Fc–coated PDMS membranes for 5 h in the presence of 16G3 antibody. (*B*) Normalized E-cadherin band intensities obtained from Co-IP measurements in panel *A* (n = 3). (*C*) Co-IP results obtained with confluent A-431D$^{E\text{-}cad}$ cells on fibronectin-coated PDMS. (*D*) Normalized E-cadherin band intensities for measurements shown in *C* (n = 3). Error bars are SEM. *P < 0.05, **P < 0.005, ***P < 0.0005.

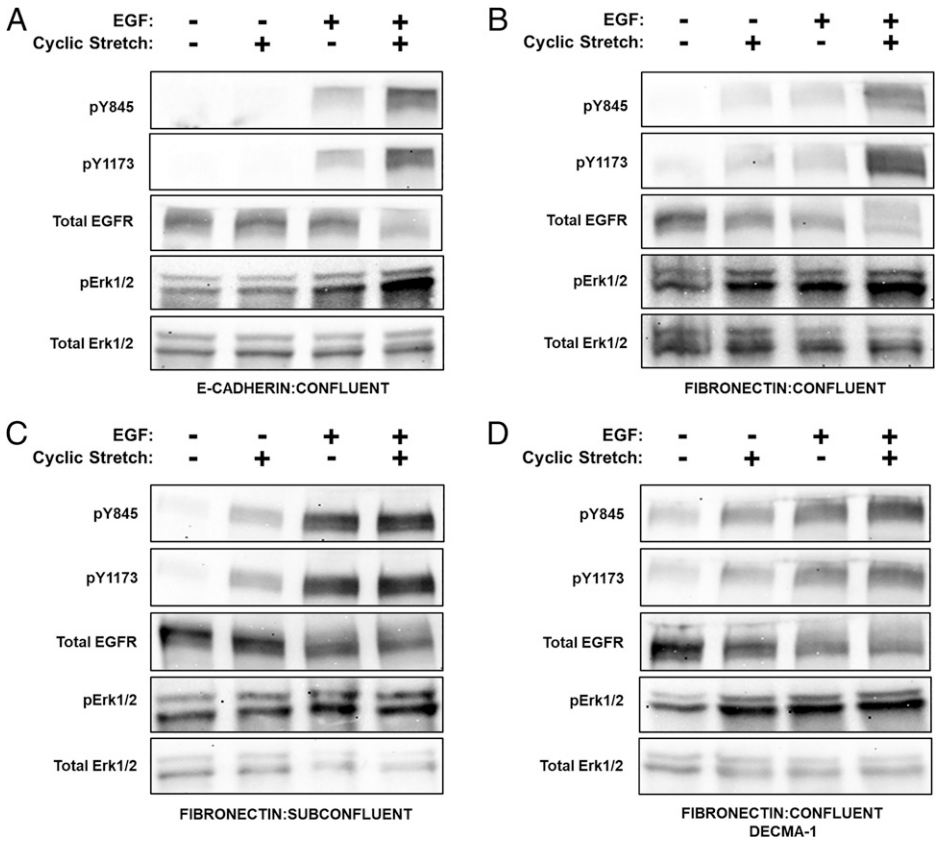

Fig. 4. E-cadherin and integrins cooperate to activate EGFR and downstream Erk1/2 in mechanically perturbed epithelia. In panels *A*–*D*, cells were subjected to four conditions: ±10% cyclic stretch and ±3 nM EGF for 30 min followed by Western blot analysis of pY845, pY1173, total EGFR, pErk1/2, and total Erk1/2. Cells were serum starved overnight, and EGF-neutralizing antibody was applied to all non–EGF-treated samples. (*A*) A-431D$^{E\text{-}cad}$ cells were plated at monolayer density on E-cad-Fc–coated PDMS membranes and allowed to attach for 5 h in the presence of 16G3 antibody. (*B*) A-431D$^{E\text{-}cad}$ cells seeded on fibronectin-coated PDMS membranes at confluent density. (*C*) A-431D$^{E\text{-}cad}$ cells were plated on fibronectin-coated PDMS membranes for 5 h at subconfluent cell density to prevent cell–cell contacts. (*D*) Confluent A-431D$^{E\text{-}cad}$ monolayers on fibronectin-coated PDMS membranes at monolayer density were serum starved overnight. Cells were treated with DECMA-1 for 30 min to disrupt cell–cell junctions.

(Fig. 4*A*). EGFR phosphorylation was assessed at Y845 and Y1173—two sites that are phosphorylated upon EGF ligation (30).

Stretching confluent A-431D$^{E\text{-}cad}$ monolayers on E-cad-Fc, in the absence of EGF, did not detectably increase pY1173 or pY845 (Fig. 4*A*). MCF-10A cells on E-cad-Fc behaved similarly (*SI Appendix*, Fig. S3). The addition of 3 nM EGF increased EGFR phosphorylation in both stretched and unstretched monolayers (Fig. 4*A*). The largest increases were in stretched cells exposed to EGF. The similar results obtained with fibronectin-blocking 16G3 antibody or control nonblocking isotype 13G12 (*SI Appendix*, Fig. S4) ruled out integrin interference. Thus, E-cadherin tension cooperates with EGF to enhance EGFR activation. Results obtained with a human EGFR phosphorylation array (*SI Appendix*, Fig. S5) confirmed the EGFR phosphorylation patterns for EGF-treated cells, with and without stretch.

Fig. 4*B* compares EGFR phosphorylation in serum-starved, confluent A-431D$^{E\text{-}cad}$ monolayers on fibronectin, under four conditions: with/without stretch and with/without 3 nM EGF. In the absence of EGF, cyclic stretch increased EGFR phosphorylation at Y845 and Y1173 relative to unstretched controls. The difference between stretched monolayers on fibronectin (Fig. 4*B*) versus on E-cad-Fc (Fig. 4*A*) is attributed to EGF-independent, integrin-mediated EGFR activation (43). Treating unstretched monolayers with 3 nM EGF further increased EGFR phosphorylation (Fig. 4*B*), as expected (43). However, cell stretching in the presence of EGF enhanced EGFR phosphorylation relative to EGF or stretch alone.

In stretched, confluent monolayers on fibronectin (Figs. 2*A* and 4*B*), both E-cadherin and integrins contribute to EGFR activation. The contribution of junctional E-cadherin to stretch-dependent EGFR activation was highlighted in two scenarios where E-cadherin adhesions were disrupted: subconfluent monolayers (Fig. 2*C*) and confluent monolayers treated with E-cadherin blocking antibody, DECMA-1 (Fig. 2*D*) (44). In the absence of EGF, cyclically stretching either subconfluent A-431D$^{E\text{-}cad}$ cells (Fig. 4*C*) or DECMA-1–treated, confluent monolayers (Fig. 4*D*) increased EGFR phosphorylation. EGFR activation in the absence cadherin adhesions is attributed to integrins. Treating unstretched, serum-starved cells with 3 nM EGF increased pY845 and pY1173 levels in both subconfluent and DECMA-1–treated cells (Fig. 4*C* and *D*). The total EGFR also decreased slightly, due to ligation-dependent internalization (45). However, EGF treatment of stretched, subconfluent cells or DECMA-1–treated monolayers on fibronectin did not further increase phosphorylated EGFR (pEGFR) levels (Fig. 4*C* and *D*). This contrasted with monolayers with intact junctions (Fig. 4*A* and *B*). *SI Appendix*, Fig. S6 summarizes the quantified, normalized changes in pEGFR levels.

Comparisons of confluent monolayers on fibronectin without (Fig. 4*B*) and with (Fig. 4*D*) DECMA-1 treatment highlight two important differences. First, added EGF resulted in a much greater increase in pEGFR in DECMA-1–treated cells (*SI Appendix*, Fig. S6*D*). Second, in confluent monolayers with intact cadherin junctions, cyclic stretch and EGF treatment nearly doubled pEGFR levels (Fig. 4*B* and *SI Appendix*, Fig. S6*B*), in

BIOPHYSICS AND COMPUTATIONAL BIOLOGY

contrast to the much smaller stretch-dependent change in either subconfluent or DECMA-1–treated monolayers (Fig. 4 *C* and *D* and *SI Appendix*, Fig. S6 *C* and *D*). We attribute the difference to contributions from stressed E-cadherin adhesions.

Force-Dependent EGFR Phosphorylation Triggers Downstream Erk1/2 Activation. We next assessed whether EGFR activation triggered the mitogen activated protein kinase (MAPK) pathway, which is a downstream effector pathway of EGFR. Fig. 4*A* and *B* compare normalized pErk1/2 levels in confluent monolayers on either E-cad-Fc (Fig. 4*A* and *SI Appendix*, Fig. S6*E*) or fibronectin (Fig. 4*B* and *SI Appendix*, Fig. S6*E*). With cells on E-cad-Fc substrates, cyclic stretch failed to increase pErk1/2 levels in the absence of EGF. Soluble EGF increased pErk1/2, and cell stretching further increased Erk1/2 activation. Different from cells on E-cad-Fc, cyclically stretching EGF-depleted cells on fibronectin triggered statistically significant increases in pErk1/2 relative to unstretched monolayers. EGF addition alone increased pErk1/2 levels, but stretch together with EGF triggered the largest increase. These results correspond with changes in pEGFR levels, under identical conditions. Treating confluent A-431D$^{E\text{-}cad}$ cells on E-cad-Fc substrates with 15 μM Gefitinib abolished both EGFR levels (*SI Appendix*, Fig. S7 *A* and *B*) and pErk1/2 (*SI Appendix*, Fig. S7 *A* and *C*), confirming that Erk1/2 phosphorylation in these assays is downstream from EGFR. Thus E-cadherin and integrins contribute to stretch-activated Erk1/2 phosphorylation in confluent cells on fibronectin, but the E-cadherin–dependent contribution requires EGF.

In subconfluent monolayers on fibronectin (Fig. 4*C* and *SI Appendix*, Fig. S6*F*) or in DECMA-1 –treated (Fig. 4*D* and *SI Appendix*, Fig. S6*F*) confluent monolayers on fibronectin, stretch or EGF independently increase pErk1/2 levels. However, in contrast to cells with intact cadherin adhesions (Fig. 4 *A* and *B* and *SI Appendix*, Fig. S6*E*), stretch and EGF do not additively enhance signaling (*SI Appendix*, Fig. S6*F*). Thus, cyclic stretch, together with EGF, activate the greatest pErk1/2 levels but only in confluent monolayers on fibronectin with intact E-cadherin adhesions (Fig. 4*B* and *SI Appendix*, Fig. S6 *E* and *F*).

E-Cadherin and EGFR Form an EGF-Sensitive Heterotrimer at the Plasma Membrane. The Co-IP results indicate that E-cadherin and EGFR are involved in complexes that are disrupted by force and/or by soluble EGF, but molecular details of the complex, such as the complex size and receptor stoichiometry, are still unknown. To address this, we used FSI-FRET (35, 46) to characterize E-cadherin interactions with EGFR at the surfaces of HEK293T cells, which do not express endogenous E-cadherin and express very little EGFR (47). The FSI-FRET method measures the FRET efficiency, donor concentration (EGFR-mTurquoise), and acceptor concentration (E-cadherin-eYFP) in the plasma membranes of live cells. We measured the FRET between EGFR and E-cadherin under four conditions: 1) absence of ligand and addition of 2) 1 nM EGF, 3) 10 nM EGF , and 4) 100 nM EGF. The measured FRET efficiencies are plotted as a function of E-cadherin-eYFP (acceptor) expression (Fig. 5 *A–D*), while *SI Appendix*, Fig. S8 displays the expression levels of E-cadherin and EGFR on individual cells in the population. At least 100 cells were imaged and analyzed for each condition: without EGF (516 cells), 1 nM EGF (393 cells), 10 nM EGF (176 cells), and 100 nM EGF (209 cells).

The FSI-FRET data demonstrate that E-cadherin directly associates with EGFR in the absence of EGF. The black curve (Fig. 5 *A–D*) is the monomer "proximity FRET," which is the FRET efficiency that would occur if the donor and acceptor by chance approached within 10 nm (48). FRET efficiencies that exceed the modeled monomer proximity curve indicate direct receptor interactions (49). In the absence of EGF, the measured distribution of FRET efficiencies deviated significantly from the proximity FRET (Fig. 5*A* and *SI Appendix*, Fig. S8*A*), indicating complex formation. Fig. 5*E* plots the deviations of the FRET efficiency from the proximity curve as a function of EGF concentration. The statistical significance of the deviations is summarized in *SI Appendix*, Table S1.

To determine the most probable oligomeric state (monomer, dimer, trimer, etc.) of the heteroreceptor complex and the receptor stoichiometry consistent with the data, all FRET data (Fig. 5 *A–D*) were globally fit to different oligomerization models (*Materials and Methods* and *SI Appendix*, *Methods*). Both E-cadherin and EGFR form homodimers at the plasma membrane (49–52), so we considered the following models in the analyses: no heterointeractions, heterodimer ($n = 2$; E-cad+EGFR) (Fig. 6*A*), heterotrimer of one EGFR and two E-cadherins ($n = 3$; EGFR+2 E-cad) (Fig. 6*B*), heterotrimer of two EGFR and one E-cadherin ($n = 3$; 2 EGFR+Ecad) (Fig. 6*C*), and a heterotetramer of two EGFR and two E-cadherins ($n = 4$; 2 EGFR + 2 Ecad) (Fig. 6*D*).

The model fit that gives the lowest mean square error (MSE) indicates the most probable complex size (oligomer order, n) and receptor stoichiometry. As shown in Fig. 5*F*, the minimum MSE determined for the E-cadherin/EGFR complex in the absence of EGF corresponds to an oligomer of order of 3 (heterotrimer) that consists of an EGFR monomer in complex with two E-cadherin proteins (Fig. 6*B*).

Soluble EGF Disrupts the Heterotrimeric E-Cadherin/EGFR Complex. The influence of soluble EGF on the complex was investigated by conducting FSI-FRET measurements with cells treated with EGF at concentrations below and above the 2 nM K_d for EGFR; namely, 1 nM, 10 nM, and 100 nM. At 1 nM EGF (Fig. 5*B* and *SI Appendix*, Fig. S8*B*), the deviation of FRET efficiencies from the proximity FRET (baseline) is statistically similar to that of untreated cells (Fig. 5 *A* and *E* and *SI Appendix*, Fig. S8*A*). Thus 1 nM EGF, which is below the K_d for EGFR, does not significantly affect the E-cadherin/EGFR complex.

Soluble EGF concentrations above the K_d for EGFR significantly decrease heterocomplex levels. In the presence of 10 nM EGF or 100 nM EGF, the FRET efficiencies "straddle" the proximity curve (Fig. 5 *C* and *D*), and the deviation from the proximity FRET shifts closer to zero (Fig. 5*E* and *SI Appendix*, Fig. S8 *C* and *D*). The distribution of acceptors and donors are similar under both conditions (*SI Appendix*, Fig. S8). The change in FRET efficiencies in Fig. 5 *C* and *D* is thus due to a decrease in E-cadherin/EGFR association. MSE analysis was performed on the FSI-FRET data in the presence of EGF at concentrations above the K_d by combining the data collected at 10 nM and 100 nM EGF and fitting to each of the hetero-interaction models (Fig. 6). We find that the MSE is minimized for the "no hetero-interaction" model ($n = 1$) (Fig. 5*F*). The EGF-dependent complex disruption is not due to EGFR internalization because the disruption of caveolae and actin upon osmotic swelling used in FSI-FRET measurements impedes endocytosis (53, 54). Also, EGFR cannot disrupt the interaction by phosphorylating proteins in the complex (55, 56) because the EGFR construct used for these FRET measurements lacks the kinase domain. These results thus show that two E-cadherin proteins bind an EGFR monomer, and soluble EGF at concentrations above the K_d for EGFR significantly reduce heteroreceptor complex levels.

Discussion

Increased tension in epithelia promotes proliferation and sensitizes cells to lower EGF concentrations, and such responses have been linked to increased force on intercellular adhesions. The present results shed light on a E-cadherin force transduction mechanism that directly links E-cadherin perturbations to EGFR activation. Co-IP and FRET data show that E-cadherin and

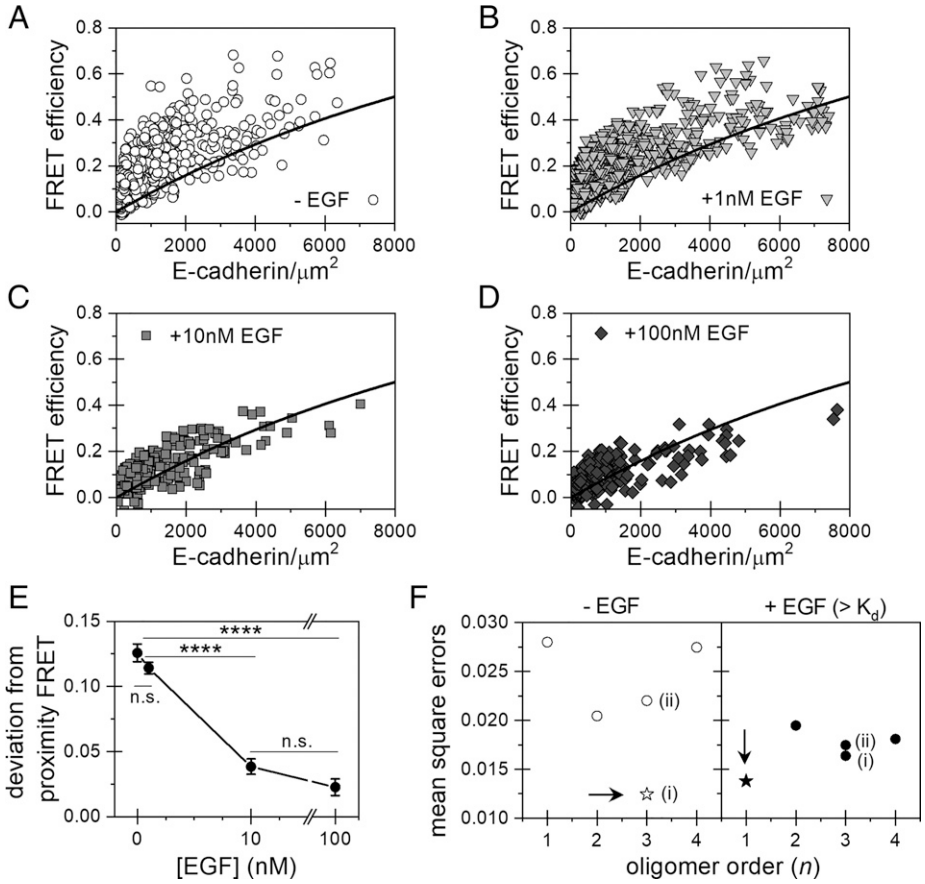

Fig. 5. FSI-FRET measurements of E-cadherin interactions with EGFR, in the absence and presence of different concentrations of EGF. (*A–D*) Plot of the E-cadherin/EGFR FRET efficiencies versus surface E-cadherin concentrations in the absence (*A*) or presence of (*B*) 1 nM, (*C*) 10 nM, (*D*) or 100 nM of EGF. The black curve is the proximity FRET void of specific interactions (48). Data *Above* the line are indicative of direct receptor interactions. (*E*) The FRET efficiencies were corrected for the contribution of the modeled proximity FRET and represented as the deviation from the proximity FRET. The deviations from the proximity FRET were calculated and plotted as histograms (*SI Appendix*, Fig. S8). The mean values and SEs are plotted as a function of EGF concentration. Errors that are not visible are smaller than the size of the symbol. Significance was calculated by ANOVA. (****$P < 0.0001$ and n.s., $P \geq 0.05$). (*F*) MSEs calculated by comparing various hetero-oligomerization models with the FRET data. The model which minimizes the MSE is the most probable complex size and stoichiometry, indicated as a star and by an arrow. The two different heterotrimer models are (*i*) one EGFR and two E-cadherin or (*ii*) two EGFR and one E-cadherin.

EGFR form complexes. Mechanically perturbing homophilic E-cadherin adhesions or treatment with EGF at concentrations above the K_d for EGFR are independently sufficient to disrupt the complex, but their combined effects are additive. Importantly, increased E-cadherin tension alone disrupts the heteroreceptor complex, but different from integrins, EGF is required for cadherin-dependent activation of EGFR and downstream Erk1/2. These results support a model in which increased force on homophilic E-cadherin bonds disrupts the complex, thereby releasing EGFR monomers to bind EGF and signal (Fig. 6*E*).

Findings also suggest that force transduction involves direct interactions between the receptors. Despite prior evidence that E-cadherin associates with EGFR, these FSI-FRET results now reveal that E-cadherin and EGFR form a heterotrimeric complex, in which two E-cadherin proteins bind an EGFR monomer (Figs. 5*F* and 6*B*). This heterotrimeric stoichiometry has potentially important mechanistic implications. EGF-dependent signaling requires EGFR homodimerization (57). The FSI-FRET results suggest that E-cadherin may inhibit EGFR by sequestering EGFR monomers, thus impairing homodimerization and signaling. EGF could disrupt the complex by shifting the equilibrium (Fig. 6*C*) to more stable EGFR homodimers or by allosterically regulating the E-cadherin/EGFR interaction. The heterocomplex stoichiometry might explain, in part, reports that E-cadherin reduces the apparent affinity between EGF and EGFR (32). These results further suggest how intercellular tension overrides contact-inhibited cell proliferation to potentiate EGFR signaling in epithelia. The mechanically activated release of EGFR suggests how junctional tension sensitizes epithelia to lower concentrations of EGF relative to unstressed tissues (8).

FSI-FRET and Co-IP results show that E-cadherin/EGFR complex formation does not require cell–cell adhesion. The dependence of EGFR inhibition on cell density could be explained by the formation of dense cadherin clusters at intercellular contacts (58, 59). Cadherin clusters are EGFR sinks with a high local density of binding sites. Physical models show that ligand (i.e., EGF) association with cadherin clusters reduces mobility at the cell surface, as well as the rate of dissociation from the clusters (60), similar to experimental observations of EGFR at intercellular adhesions (34).

Importantly, given the complexity of cell membranes and differences between cells, other factors may affect E-cadherin/EGFR complexes. For example, Her2 (ERBB2) heterodimerizes with EGFR (61), and it also binds E-cadherin ectodomains (62, 63); thus competitive Her2 association with either E-cadherin or EGFR monomers could alter E-cadherin/EGFR levels. Interactions with the cytoskeleton and Merlin could also augment heterocomplex stability by impeding EGFR diffusion

BIOPHYSICS AND COMPUTATIONAL BIOLOGY

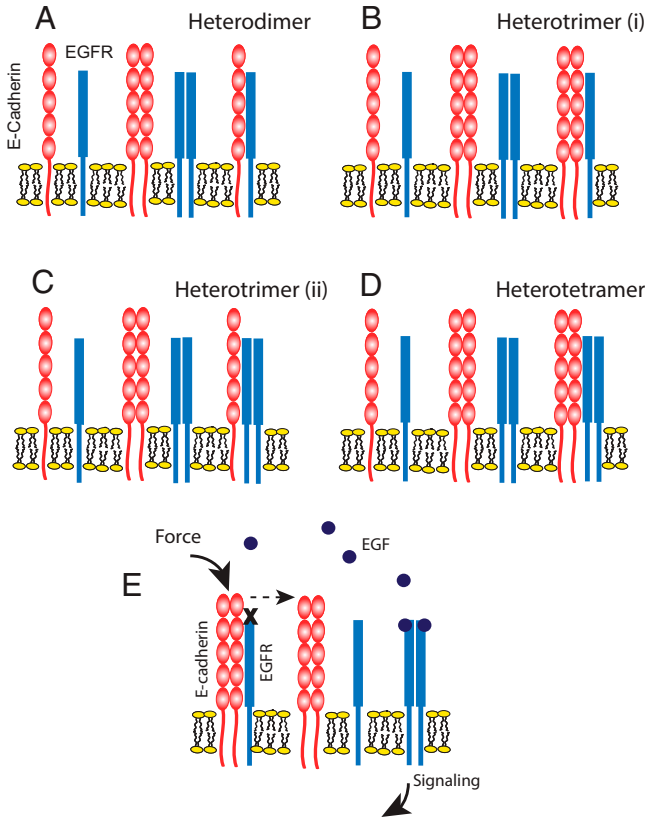

Fig. 6. Cartoon representations of the hetero-interaction models considered for the E-cadherin/EGFR complex and proposed mechanism of force-activated EGFR signaling. (*A*) Heterodimer model consisting of one E-cadherin and one EGFR molecule. (*B*) Heterotrimer (*i*) model consisting of two E-cadherins and one EGFR. (*C*) Heterotrimer (*ii*) model consisting of one E-cadherin and two EGFR molecules. (*D*) Heterotetramer model consisting of two E-cadherin and two EGFR molecules. (*E*) Proposed model of E-cadherin/EGFR complex formation and EGFR activation by mechanically perturbing E-cadherin receptors. E-cadherin homodimers sequester EGFR monomers at the plasma membrane. Applied force on homophilic E-cadherin bonds triggers EGFR dissociation and frees EGFR monomers to dimerize, bind EGF ligand, and signal. Soluble EGF can also disrupt the complex by shifting the equilibrium in favor of the more stable, ligand-bound EGFR state.

and internalization (34, 38). Factors such as lipids that affect EGFR clustering and signaling (64) may also play a role. These are important issues, but the results presented here open avenues for pursuing such questions.

Here, results directly connect mechanical perturbations of homophilic E-cadherin bonds to EGFR release as a first step in force transduction signaling. The results do not reveal how force disrupts the complex, but there are hints. Prior studies similarly demonstrated that tugging alone did not activate cadherin force transduction, but tugging with homophilic ligands did (24, 40, 41). Both cadherins and EGFR are allosteric proteins (61, 65, 66); thus homophilic E-cadherin ligation may allosterically regulate E-cadherin/EGFR binding.

This study did not focus on identifying the E-cadherin/EGFR binding interface. However, prior results suggest that the E-cadherin ectodomain is required for EGFR binding. Swapping the E-cadherin ectodomain with N-cadherin or deleting the ectomain both abolished E-cadherin/EGFR Co-IPs (29, 32). E-cadherin point mutants implicated in diffuse gastric cancer increase EGFR activation (67). The ectodomain requirement differs from evidence that the transmembrane domain of vascular endothelial cadherin mediates binding to vascular endothelial growth factor receptors 2/3 (68). Future FSI-FRET measurements will identify regions of EGFR and E-cadherin that mediate heterocomplex formation and establish whether E-cadherin dimers (52, 69) are required.

Integrins and E-cadherin both mechanically activate EGFR in cyclically stretched epithelia by distinctly different mechanisms. E-cadherin–mediated force transduction involves EGF-dependent EGFR activation (24, 25). Force disrupts E-cadherin/EGFR complexes, independent of EGF to potentiate EGFR signaling. By contrast, integrins activate EGFR by an EGF-independent mechanism involving Src (43, 70). Thus both cadherins and integrins simultaneously contribute to stretch-activated growth factor receptor signaling in epithelia, with the greatest activation in EGF-treated monolayers with intact cell–cell junctions.

These findings directly link E-cadherin mechanotransduction to proproliferative signaling. E-cadherin force transduction activates phosphoinositide-3′-kinase (PI3K) and Akt (24, 25)—two factors in pathways that regulate proliferation and survival. Other results showed that Yap1 and β−catenin activation in mechanically strained epithelia promote cell cycle reentry (9). In the latter study, upstream force transduction events were not identified, but other findings suggest possible links to results in this study. Junctional tension activates a conformational change in α−catenin that recruits Ajuba proteins, which inhibit LATS1/2 and downstream Yap1 activation (6, 7, 13). Our results demonstrate that stressed E-cadherin adhesions activate EGFR and downstream Erk1/2, which is a well-known regulator of cell proliferation through multiple mechanisms, including the phosphorylation of Ajuba proteins (31). Additionally, phosphorylation by Akt downstream from EGFR increases β−catenin transcriptional activity (9). Establishing connections between the mechano-activation of EGFR at E-cadherin junctions and the regulation of Hippo and β−catenin/Wnt signaling would provide further insight into the mechanical regulation of epithelial cell proliferation and organ growth.

Materials and Methods

Cells. For FSI-FRET experiments, we used HEK293T cells, which do not express endogenous E-cadherin and very little EGFR (47). These cells were transiently transfected with plasmids that encoded EGFR or E-cadherin, in which the intracellular domains were substituted with fluorescent proteins, mTurquoise (mTurq), or enhanced yellow fluorescent protein (eYFP) that were attached by a flexible $(GGS)_5$ linker.

Studies of E-cadherin/EGFR interactions in mechanically stretched epithelial cells used A-431D epidermoid carcinoma cells that were engineered to stably express the full-length human E-cadherin (A-431D^{Ecad}) with a C-terminal green fluorescent protein (GFP) (deposited by Dr. Jennifer Stow, Addgene plasmid, 28009) (71). The A-431D line (from Prof. Keith Johnson, University of Nebraska) over expresses EGFR but does not express endogenous classical cadherins (36). Cell stretching studies were also done with MCF10A cells, which express typical levels of E-cadherin and EGFR. HEK293T cells were not used in stretching studies because they do not form intact monolayers. Conversely, A-431D cells were not used for FSI-FRET measurements because they express endogenous EGFR.

FSI-FRET Measurements. FSI-FRET measurements were carried out as described (35, 50), by imaging single cells under reversible osmotic stress. A mode-locked laser (MaiTai, Spectra-Physics) that generates femtosecond pulses between wavelengths 690 to 1,040 nm was used to excite the fluorophores (72, 73). Each cell was imaged twice, at the wavelengths of 840 and 960 nm, to excite the donor and the acceptor, respectively (72, 73). Only regions of the cell membrane not in contact with neighboring cells, far from intercellular junctions, were imaged. The concentrations of membrane receptors in the plasma membrane were quantified with a calibration curve that was generated with solutions of purified fluorescent proteins (35). The fluorescent proteins, mTurquoise and eYFP, were produced as described (74), and solutions of each were made at known 3D concentrations and imaged at the wavelengths of 840 and 960 nm. Linear calibration curves of the pixel-level intensities versus the known concentrations were generated in order to convert the effective 3D protein concentration into two-dimensional protein concentrations at the plasma membrane (35, 75). Thus for each selected region of the cell

membrane, we calculated the FRET efficiency, donor concentration, and acceptor concentration (35). These data from >100 cells were then fit to different receptor oligomerization models to identify the oligomerization state (monomer, dimer, trimer, etc.) and the stoichiometry of receptors in the complex.

Hetero-interaction models were fit to the experimental FRET data using a two-step process. The fits identified the optimal values for the two unknown parameters: the association constant (K) and the Intrinsic FRET ($\tilde{E}$). In the first step, the value of the Intrinsic FRET was fixed, and a nonlinear least squares fit determined the association constant. This process was repeated at discreet values of $\tilde{E}$ in 0.01 increments. Then in the second step, the MSE was calculated for each of the resulting pairs of $\tilde{E}$ and K values. The values of $\tilde{E}$ and K that minimize the MSE value are considered the best-fit values for that particular model. This entire process is repeated for each heterointeraction model (Fig. 6 *A*–*D*), and the resulting MSE values are compared in Fig. 5*E*. More details of the measurements and analyses, as well as the models and data fitting are in *SI Appendix, Methods*.

Cell Stretching. Cell monolayers were mechanically perturbed with a home-built cell-stretcher, described previously (76). Cells were seeded on protein-coated, elastomeric, PDMS membranes in the configurations shown in Fig. 2 *A*–*D*. The PDMS coatings and experimental conditions are described in detail in *SI Appendix, Methods*.

Co-IP and Western Blots. Co-IP measurements of E-cadherin and EGFR were conducted using standard procedures. Immunoprecipitated proteins were identified by Western blot after separation by sodium dodecylsulfate polyacrylamide gel electrophoresis. Monoclonal, rat anti-EGFR antibody (Cell Signaling Technology, 4267) was used for Western blots of EGFR and for immunoprecipitation. Polyclonal, anti-phospho-EGFR (Tyr845) antibody (Fisher Scientific, 44-784G) and monoclonal phospho-EGFR (Tyr1173) antibody (Cell Signaling Technology, 4407) was used to detect EGFR phosphorylation. EGFR phosphorylation was also assessed with an EGFR phosphorylation array (Ray Biotech). Immunoblots and immunoprecipitation measurements of E-cadherin used monoclonal anti–E-cadherin (Fisher Scientific, BDB610181). Phospho-Erk1/2 and total Erk1/2 were detected with polyclonal phospho-p44/42 MAPK antibody (Cell Signaling Technology, 9101S) and monoclonal p44/42 MAPK antibody (Cell Signaling Technology, 4695). Additional details are in *SI Appendix, Materials* and *Methods*.

Statistical Analysis. In FSI-FRET measurements, more than 100 cells were analyzed per condition. The significance for FSI-FRET measurements was calculated by ANOVA and a Tukey test for multiple comparisons using the GraphPad Prism 8 software. A $P < 0.05$ was set as the standard for significance (n.s. indicates $P \geq 0.05$, * indicates $P = 0.01$ to 0.05, ** indicates $P = 0.001$ to 0.01, *** indicates $P = 0.0001$ to 0.001, and **** indicates $P < 0.0001$). Bartlett's test was used to confirm the homogeneity of the variances across the data sets.

Band intensities in Western blots were analyzed with ImageJ software. The relative band intensities for the Co-IP assays and for EGFR and Erk1/2 phosphorylation assays were calculated with Microsoft Excel. *P* values were calculated using the two-tailed Student's *t* tests, with $P < 0.05$ as the standard for significance. The SEM was calculated from the SD between sample sets and was included in all the relative intensity graphs for the immunoblots. Results acquired represent a minimum of three experimental replicates for statistical analysis. Additional information is provided in the text and figure legends.

Data Availability. All data included in the article and/or *SI Appendix*.

ACKNOWLEDGMENTS. This work was supported by the NIH under Grant No. 5 RO1GM127554-01 to K.H. and D.L. We thank Dr. Sandy McMaster for preparing the culture media and Saiko Rosenberger for technical assistance.

1. M. Marsden, D. W. DeSimone, Integrin-ECM interactions regulate cadherin-dependent cell adhesion and are required for convergent extension in Xenopus. *Curr. Biol.* **13**, 1182–1191 (2003).
2. T. Hayashi, R. W. Carthew, Surface mechanics mediate pattern formation in the developing retina. *Nature* **431**, 647–652 (2004).
3. J. D. Humphrey, E. R. Dufresne, M. A. Schwartz, Mechanotransduction and extracellular matrix homeostasis. *Nat. Rev. Mol. Cell Biol.* **15**, 802–812 (2014).
4. J. Huynh *et al.*, Age-related intimal stiffening enhances endothelial permeability and leukocyte transmigration. *Sci. Transl. Med.* **3**, 112ra122 (2011).
5. E. Tzima *et al.*, A mechanosensory complex that mediates the endothelial cell response to fluid shear stress. *Nature* **437**, 426–431 (2005).
6. C. Rauskolb, S. Sun, G. Sun, Y. Pan, K. D. Irvine, Cytoskeletal tension inhibits Hippo signaling through an Ajuba–Warts complex. *Cell* **158**, 143–156 (2014).
7. C. Ibar *et al.*, Tension-dependent regulation of mammalian Hippo signaling through LIMD1. *J. Cell Sci.* **131**, jcs214700 (2018).
8. J. H. Kim, A. R. Asthagiri, Matrix stiffening sensitizes epithelial cells to EGF and enables the loss of contact inhibition of proliferation. *J. Cell Sci.* **124**, 1280–1287 (2011).
9. B. W. Benham-Pyle, B. L. Pruitt, W. J. Nelson, Cell adhesion. Mechanical strain induces E-cadherin-dependent Yap1 and β-catenin activation to drive cell cycle entry. *Science* **348**, 1024–1027 (2015).
10. A. Mohan *et al.*, Spatial proliferation of epithelial cells is regulated by E-cadherin force. *Biophys. J.* **115**, 853–864 (2018).
11. V. Narayanan *et al.*, Osmotic gradients in epithelial acini increase mechanical tension across E-cadherin, drive morphogenesis, and maintain homeostasis. *Curr. Biol.* **30**, 624–633.e4 (2020).
12. S. Sun, K. D. Irvine, Cellular organization and cytoskeletal regulation of the Hippo signaling network. *Trends Cell Biol.* **26**, 694–704 (2016).
13. H. Alégot *et al.*, Recruitment of Jub by α-catenin promotes Yki activity and *Drosophila* wing growth. *J. Cell Sci.* **132**, jcs222018 (2019).
14. A. Katsumi, A. W. Orr, E. Tzima, M. A. Schwartz, Integrins in mechanotransduction. *J. Biol. Chem.* **279**, 12001–12004 (2004).
15. A. D. Bershadsky, N. Q. Balaban, B. Geiger, Adhesion-dependent cell mechanosensitivity. *Annu. Rev. Cell Dev. Biol.* **19**, 677–695 (2003).
16. S. Yonemura, Y. Wada, T. Watanabe, A. Nagafuchi, M. Shibata, alpha-Catenin as a tension transducer that induces adherens junction development. *Nat. Cell Biol.* **12**, 533–542 (2010).
17. D. E. Leckband, J. de Rooij, Cadherin adhesion and mechanotransduction. *Annu. Rev. Cell Dev. Biol.* **30**, 291–315 (2014).
18. C. M. Niessen, D. Leckband, A. S. Yap, Tissue organization by cadherin adhesion molecules: Dynamic molecular and cellular mechanisms of morphogenetic regulation. *Physiol. Rev.* **91**, 691–731 (2011).
19. M. Takeichi, Morphogenetic roles of classic cadherins. *Curr. Opin. Cell Biol.* **7**, 619–627 (1995).
20. B. M. Gumbiner, Cell adhesion: The molecular basis of tissue architecture and morphogenesis. *Cell* **84**, 345–357 (1996).
21. J. M. Halbleib, W. J. Nelson, Cadherins in development: Cell adhesion, sorting, and tissue morphogenesis. *Genes Dev.* **20**, 3199–3214 (2006).
22. L. Shapiro, W. I. Weis, Structure and biochemistry of cadherins and catenins. *Cold Spring Harb. Perspect. Biol.* **1**, a003053 (2009).
23. Q. le Duc *et al.*, Vinculin potentiates E-cadherin mechanosensing and is recruited to actin-anchored sites within adherens junctions in a myosin II-dependent manner. *J. Cell Biol.* **189**, 1107–1115 (2010).
24. I. Muhamed *et al.*, E-cadherin-mediated force transduction signals regulate global cell mechanics. *J. Cell Sci.* **129**, 1843–1854 (2016).
25. P. Sehgal *et al.*, Epidermal growth factor receptor and integrins control force-dependent vinculin recruitment to E-cadherin junctions. *J. Cell Sci.* **131**, jcs206656 (2018).
26. N. G. Kim, E. Koh, X. Chen, B. M. Gumbiner, E-cadherin mediates contact inhibition of proliferation through Hippo signaling-pathway components. *Proc. Natl. Acad. Sci. U.S.A.* **108**, 11930–11935 (2011).
27. A. I. McClatchey, A. S. Yap, Contact inhibition (of proliferation) redux. *Curr. Opin. Cell Biol.* **24**, 685–694 (2012).
28. M. Perrais, X. Chen, M. Perez-Moreno, B. M. Gumbiner, E-cadherin homophilic ligation inhibits cell growth and epidermal growth factor receptor signaling independently of other cell interactions. *Mol. Biol. Cell* **18**, 2013–2025 (2007).
29. X. Qian, T. Karpova, A. M. Sheppard, J. McNally, D. R. Lowy, E-cadherin-mediated adhesion inhibits ligand-dependent activation of diverse receptor tyrosine kinases. *EMBO J.* **23**, 1739–1748 (2004).
30. B. M. Gumbiner, N. G. Kim, The Hippo-YAP signaling pathway and contact inhibition of growth. *J. Cell Sci.* **127**, 709–717 (2014).
31. B. V. Reddy, K. D. Irvine, Regulation of Hippo signaling by EGFR-MAPK signaling through Ajuba family proteins. *Dev. Cell* **24**, 459–471 (2013).
32. M. Fedor-Chaiken, P. W. Hein, J. C. Stewart, R. Brackenbury, M. S. Kinch, E-cadherin binding modulates EGF receptor activation. *Cell Commun. Adhes.* **10**, 105–118 (2003).
33. A. R. Mateus *et al.*, E-cadherin mutations and cell motility: A genotype-phenotype correlation. *Exp. Cell Res.* **315**, 1393–1402 (2009).
34. C. Chiasson-MacKenzie *et al.*, NF2/Merlin mediates contact-dependent inhibition of EGFR mobility and internalization via cortical actomyosin. *J. Cell Biol.* **211**, 391–405 (2015).
35. C. King, M. Stoneman, V. Raicu, K. Hristova, Fully quantified spectral imaging reveals in vivo membrane protein interactions. *Integr. Biol.* **8**, 216–229 (2016).
36. J. E. Lewis *et al.*, Cross-talk between adherens junctions and desmosomes depends on plakoglobin. *J. Cell Biol.* **136**, 919–934 (1997).
37. A. R. Mateus *et al.*, EGFR regulates RhoA-GTP dependent cell motility in E-cadherin mutant cells. *Hum. Mol. Genet.* **16**, 1639–1647 (2007).
38. M. Curto, B. K. Cole, D. Lallemand, C. H. Liu, A. I. McClatchey, Contact-dependent inhibition of EGFR signaling by Nf2/Merlin. *J. Cell Biol.* **177**, 893–903 (2007).
39. R. Fan, N. G. Kim, B. M. Gumbiner, Regulation of Hippo pathway by mitogenic growth factors via phosphoinositide 3-kinase and phosphoinositide-dependent kinase-1. *Proc. Natl. Acad. Sci. U.S.A.* **110**, 2569–2574 (2013).
40. H. Tabdili *et al.*, Cadherin-dependent mechanotransduction depends on ligand identity but not affinity. *J. Cell Sci.* **125**, 4362–4371 (2012).

41. A. K. Barry, N. Wang, D. E. Leckband, Local VE-cadherin mechanotransduction triggers long-ranged remodeling of endothelial monolayers. *J. Cell Sci.* **128**, 1341–1351 (2015).
42. C. Chiasson-MacKenzie, A. I. McClatchey, Cell–cell contact and receptor tyrosine kinase signaling. *Cold Spring Harb. Perspect. Biol.* **10**, a029215 (2018).
43. M. Saxena *et al.*, EGFR and HER2 activate rigidity sensing only on rigid matrices. *Nat. Mater.* **16**, 775–781 (2017).
44. M. Ozawa, H. Hoschützky, K. Herrenknecht, R. Kemler, A possible new adhesive site in the cell-adhesion molecule uvomorulin. *Mech. Dev.* **33**, 49–56 (1990).
45. L. Henriksen, M. V. Grandal, S. L. Knudsen, B. van Deurs, L. M. Grøvdal, Internalization mechanisms of the epidermal growth factor receptor after activation with different ligands. *PLoS One* **8**, e58148 (2013).
46. N. Del Piccolo, S. Sarabipour, K. Hristova, A new method to study heterodimerization of membrane proteins and its application to fibroblast growth factor receptors. *J. Biol. Chem.* **292**, 1288–1301 (2017).
47. M. S. Brea *et al.*, Epidermal growth factor receptor silencing blunts the slow force response to myocardial stretch. *J. Am. Heart Assoc.* **5**, e004017 (2016).
48. A. H. Clayton, A. Chattopadhyay, Taking care of bystander FRET in a crowded cell membrane environment. *Biophys. J.* **106**, 1227–1228 (2014).
49. C. King, S. Sarabipour, P. Byrne, D. J. Leahy, K. Hristova, The FRET signatures of noninteracting proteins in membranes: Simulations and experiments. *Biophys. J.* **106**, 1309–1317 (2014).
50. N. Del Piccolo, K. Hristova, Quantifying the interaction between EGFR dimers and Grb2 in live cells. *Biophys. J.* **113**, 1353–1364 (2017).
51. P. O. Byrne, K. Hristova, D. J. Leahy, EGFR forms ligand-independent oligomers that are distinct from the active state. *J. Biol. Chem.* **295**, 13353–13362 (2020).
52. D. R. Singh, F. Ahmed, S. Sarabipour, K. Hristova, Intracellular domain contacts contribute to ecadherin constitutive dimerization in the plasma membrane. *J. Mol. Biol.* **429**, 2231–2245 (2017).
53. B. Sinha *et al.*, Cells respond to mechanical stress by rapid disassembly of caveolae. *Cell* **144**, 402–413 (2011).
54. J. P. Ferguson *et al.*, Mechanoregulation of clathrin-mediated endocytosis. *J. Cell Sci.* **130**, 3631–3636 (2017).
55. J. Lilien, J. Balsamo, The regulation of cadherin-mediated adhesion by tyrosine phosphorylation/dephosphorylation of beta-catenin. *Curr. Opin. Cell Biol.* **17**, 459–465 (2005).
56. D. J. Mariner, M. A. Davis, A. B. Reynolds, EGFR signaling to p120-catenin through phosphorylation at Y228. *J. Cell Sci.* **117**, 1339–1350 (2004).
57. M. A. Lemmon, J. Schlessinger, Cell signaling by receptor tyrosine kinases. *Cell* **141**, 1117–1134 (2010).
58. B. A. Truong Quang, M. Mani, O. Markova, T. Lecuit, P. F. Lenne, Principles of E-cadherin supramolecular organization in vivo. *Curr. Biol.* **23**, 2197–2207 (2013).
59. Y. Wu, P. Kanchanawong, R. Zaidel-Bar, Actin-delimited adhesion-independent clustering of E-cadherin forms the nanoscale building blocks of adherens junctions. *Dev. Cell* **32**, 139–154 (2015).
60. M. Gopalakrishnan, K. Forsten-Williams, M. A. Nugent, U. C. Täuber, Effects of receptor clustering on ligand dissociation kinetics: Theory and simulations. *Biophys. J.* **89**, 3686–3700 (2005).
61. M. A. Lemmon, J. Schlessinger, K. M. Ferguson, The EGFR family: Not so prototypical receptor tyrosine kinases. *Cold Spring Harb. Perspect. Biol.* **6**, a020768 (2014).
62. O. Shafraz, B. Xie, S. Yamada, S. Sivasankar, Mapping transmembrane binding partners for E-cadherin ectodomains. *Proc. Natl. Acad. Sci. U.S.A.* **117**, 31157–31165 (2020).
63. A. J. Najy, K. C. Day, M. L. Day, The ectodomain shedding of E-cadherin by ADAM15 supports ErbB receptor activation. *J. Biol. Chem.* **283**, 18393–18401 (2008).
64. Ü. Coskun, M. Grzybek, D. Drechsel, K. Simons, Regulation of human EGF receptor by lipids. *Proc. Natl. Acad. Sci. U.S.A.* **108**, 9044–9048 (2011).
65. N. Shashikanth *et al.*, Allosteric regulation of E-cadherin adhesion. *J. Biol. Chem.* **290**, 21749–21761 (2015).
66. Y. I. Petrova, M. M. Spano, B. M. Gumbiner, Conformational epitopes at cadherin calcium-binding sites and p120-catenin phosphorylation regulate cell adhesion. *Mol. Biol. Cell* **23**, 2092–2108 (2012).
67. K. F. Becker *et al.*, Identification of eleven novel tumor-associated E-cadherin mutations. Mutations in brief no. 215. Online. *Hum. Mutat.* **13**, 171 (1999).
68. B. G. Coon *et al.*, Intramembrane binding of VE-cadherin to VEGFR2 and VEGFR3 assembles the endothelial mechanosensory complex. *J. Cell Biol.* **208**, 975–986 (2015).
69. V. Vu *et al.*, P120 catenin potentiates constitutive E-cadherin dimerization at the plasma membrane and regulates trans binding. *Curr. Biol.* **31**, 3017–3027.e7 (2021).
70. L. Moro *et al.*, Integrin-induced epidermal growth factor (EGF) receptor activation requires c-Src and p130Cas and leads to phosphorylation of specific EGF receptor tyrosines. *J. Biol. Chem.* **277**, 9405–9414 (2002).
71. N. Shashikanth, M. A. Kisting, D. E. Leckband, Kinetic measurements reveal enhanced protein–protein interactions at intercellular junctions. *Sci. Rep.* **6**, 23623 (2016).
72. G. Biener *et al.*, Development and experimental testing of an optical microspectroscopic technique incorporating true line-scan excitation. *Int. J. Mol. Sci.* **15**, 261–276 (2013).
73. V. Raicu *et al.*, Determination of supramolecular structure and spatial distribution of protein complexes in living cells. *Nat. Photonics* **3**, 107–113 (2009).
74. S. Sarabipour, C. King, K. Hristova, Uninduced high-yield bacterial expression of fluorescent proteins. *Anal. Biochem.* **449**, 155–157 (2014).
75. L. Chen, L. Novicky, M. Merzlyakov, T. Hristov, K. Hristova, Measuring the energetics of membrane protein dimerization in mammalian membranes. *J. Am. Chem. Soc.* **132**, 3628–3635 (2010).
76. A. Dan, R. B. Huang, D. E. Leckband, Dynamic imaging reveals coordinate effects of cyclic stretch and substrate stiffness on endothelial integrity. *Ann. Biomed. Eng.* **44**, 3655–3667 (2016).